Probing the Accretion Physics of Active Galactic Nuclei with X-ray Timing Instruments

Ethan Partington [1], Edward Cackett [2], Chris Barnes [1]
[1] Western Kentucky University, [2] Wayne State University; Contact: ethan.partington@wku.edu

NICER was the first instrument able to track flux variability in the **multiple X-ray emission components** of AGN and monitor their **changing disk winds** on timescales of **days to years** via single-epoch spectral modeling.

Coordinated UV and optical monitoring enabled lag measurements that probed the geometry of the X-ray sources and the accretion disk.

Due to its improved sensitivity and reduced background, DEUS-X would probe even **shorter variability timescales** and could study even **fainter AGN**.

Probing the Disk—Corona Connection in Unobscured AGN

NICER delivered 1 ks spectra of eight AGN targets every 1-2 days, each as part of a coordinated reverberation mapping campaign with contemporaneous UV and optical monitoring.

Most of the X-ray flux in these AGN comes from inverse Compton scattering in a hot ($kT_e \sim 100$ keV), compact corona producing a power-law spectrum. Additional emission below 2 keV is known as the "soft excess." In some sources such as NGC 7469, the soft excess is attributed to the blurred reflection of hard X-rays in the inner disk,[1] also associated with the broad Fe Kα line at 6.4 keV. In others such as Fairall 9,[2] Mrk 142 and Mrk 841, additional continuum emission from an extended "warm" corona of Comptonizing electrons ($kT_e \sim 1$ keV) likely contributes to the soft excess.[2]

These experiments probed the connection between X-ray emission and the accretion disk by searching for correlated variability offset by a time lag, indicative of thermal reprocessing of the X-rays by the disk.

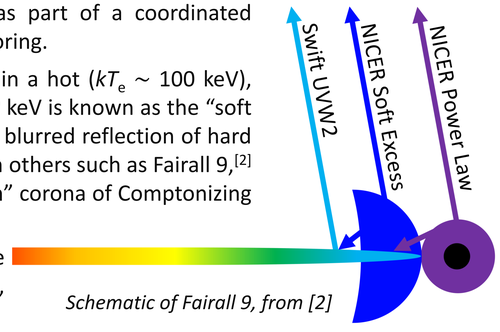

Schematic of Fairall 9, from [2]

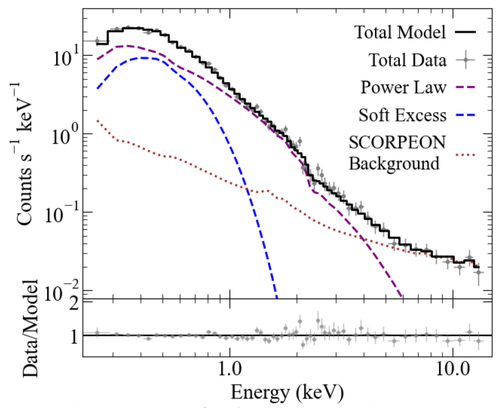

A NICER spectrum of Mrk 142 on MJD 58564, using a phenomenological blackbody model for the soft excess.

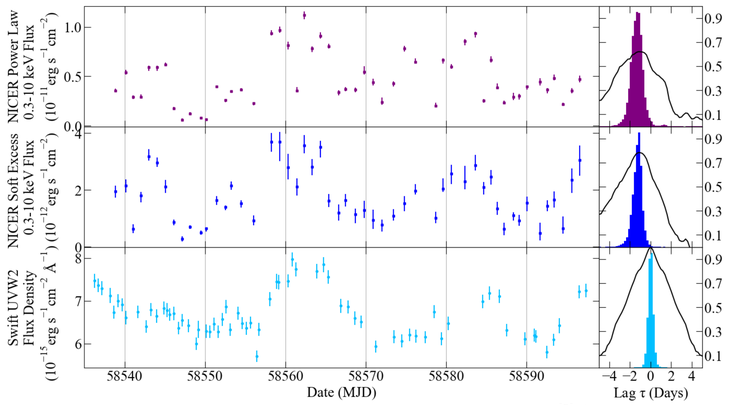

Flux light curves and Interpolated Cross-Correlation Functions [3] for Mrk 142. Negative lags indicate that the X-rays lead the UV. (Partington et al., in prep.)

The extremely soft power law continuum ($\Gamma_{median} = 2.5$) indicates cool electron temperatures in the corona. The soft excess in Mrk 142 lacks the high-frequency variability of the power law component, implying that it comes from a larger emission region. This suggests that the soft excess primarily comes from an extended warm Comptonization region around the compact corona.

Since Mrk 142 accretes at or above the Eddington limit, the inner disk is likely slim rather than geometrically thin.[22] Lags between the X-ray and UV light curves are longer than expected given the black hole's mass, which may indicate that the X-ray variability first propagates slowly through the slim inner disk which blocks direct X-ray reprocessing in the outer disk.

In three AGN, we notice much stronger correlations between variability in the soft excess and the UV than the power law and the UV, challenging the traditional idea that the hard X-rays drive fast variability in the accretion disk through reprocessing.

Lag measurements and variability timescales in these AGN suggest that the soft excess source is larger than the power law source, supporting the picture of an extended "warm corona."[9]

AGN	L_{bol}/L_{Edd}	M_{SMBH} ($\times 10^6 M_\odot$)	Power Law/UVW2 Lag (days)	Power Law/UVW2 R	Soft Excess/UVW2 Lag (days)	Soft Excess/UVW2 R
Mrk 142	0.74–3.4 [4]	1.7 [5]	$-1.3^{+0.5}_{-0.6}$	0.62	$-1.2^{+0.3}_{-0.5}$	0.78
Mrk 876	0.42 [6]	220 [7]	$-3.6^{+1.9}_{-2.2}$	0.30	$-2.9^{+1.8}_{-7.3}$	0.16
NGC 7469 [1]	0.23 [8]	9 [7]	-0.7 ± 0.5	0.77	-1.2 ± 0.5	0.77
Fairall 9 [2]	0.06 [9]	260 [10]	$0.8^{+2.8}_{-2.0}$	0.51	$-2.4^{+1.4}_{-1.0}$	0.82
			Power Law/g-band		Soft Excess/g-band	
Mrk 841	?	30–70 [12]	$-1.3^{+0.7}_{-0.9}$	0.70	$-4.2^{+1.1}_{-1.5}$	0.83

Tracking Variable Disk Winds in Mrk 817 and NGC 4151

In Mrk 817, the column density (N_H) of an ionized X-ray obscurer repeatedly increases by up to 10x and returns to a baseline $N_H \approx 10^{22}$ cm^{-2} in under 100 days. Evolution in the X-ray N_H *(purple)* is strongly correlated with the equivalent widths of blueshifted UV absorption lines measured by HST COS *(blue),* suggesting a common origin in an outflowing wind emitted from the accretion disk.[13] In March 2023, the obscuration weakened significantly, with soft X-ray fluxes returning to historical levels.

The UV obscuration disappears during the low X-ray N_H states. Since UV absorption requires much higher gas densities than X-rays do, the wind is likely a multiphase medium with a diffuse X-ray absorbing component and dense clumps. Variability in the X-ray coronal flux may create thermal instabilities in the gas as proposed by [17], causing these clumps to form.

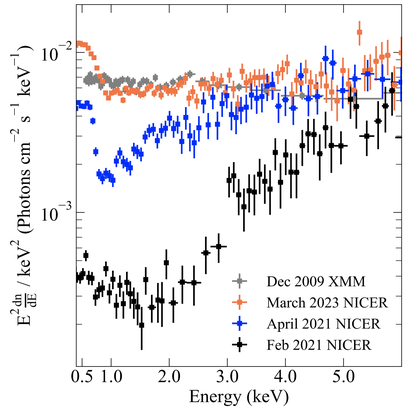

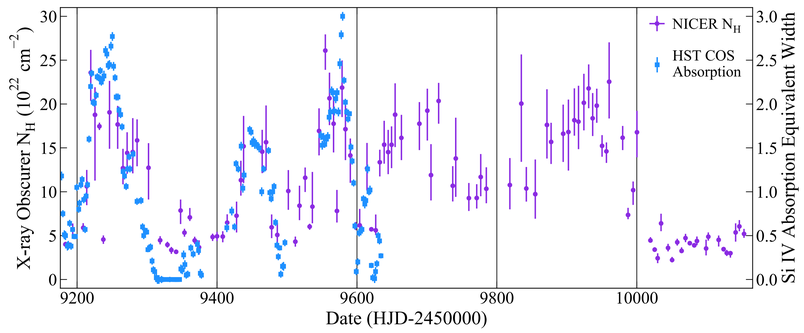

Left: Unfolded NICER spectra of Mrk 817 showing lifting obscuration from 2021-2023
Right: Evolution of the column density in Mrk 817 from 2021-2023, adapted from [13]

NICER shows that NGC 4151 also experiences strong variability in N_H on timescales of months, indicating instability in its disk winds. In both AGN, increases in the observed X-ray flux are driven by reduced obscuration plus intrinsic changes in the corona.

XRISM observations of NGC 4151 occurred during a state of powerful ultra-fast outflows.[18] Shortly after, NICER captured a decrease in the overall obscuration. This highlights the need for long-term monitoring to characterize the complicated wind systems in AGN.

AGN	L_{bol}/L_{Edd}	M_{SMBH} ($\times 10^6 M_\odot$)	Observed Flux/UVW2 R_{max}	Unobscured Flux/UVW2 R_{max}
Mrk 817 [13]	0.22 [14]	39 [14]	0.27	0.28
NGC 4151 [13]	0.01–0.1 [15]	17 [16]	0.07	0.06

Both AGN showed no significant correlation between variability in the UV and either the observed or intrinsic (unobscured) X-ray fluxes. This suggests that variable obscuration alters the driving light curve incident on the disk, disrupting direct X-ray reprocessing from the corona.[13]

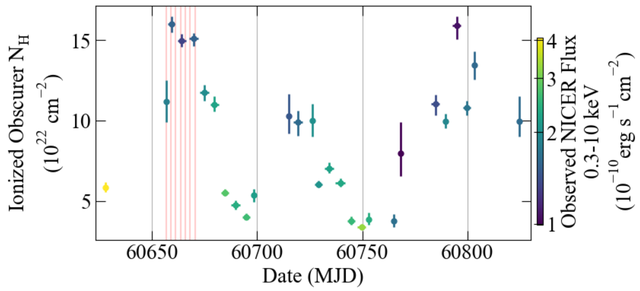

Evolution of N_H in NGC 4151, measured with NICER from 2024—2025. (Partington et al., in prep.) Red lines mark dates of XRISM observations.[18]

Unlocking New AGN Science With DEUS-X

DEUS-X would have ~ 10× the effective areas of NICER at 1.5 keV and RXTE at 6.5 keV, improving on the LEMA and HEMA designs of STROBE-X.

In a 1 ks spectrum, we would be able to constrain models of AGN absorption and emission components in ten intervals of 100 s. This would unlock more precise lag measurements, constraining the size of the X-ray emitting regions.

With improved sensitivity to the broad Fe Kα line, we could simultaneously model the contributions of relativistic reflection and warm Comptonization in the soft excess on much shorter timescales than can be done with XMM.[19] This would improve constraints on the spectral energy distributions of AGN.

DEUS-X would contain a *Swift* UVOT-like instrument, providing simultaneous UV/optical continuum flux measurements to probe the structure of the disk.

Lower background levels compared to NICER would unlock high-cadence spectral analysis of faint sources such as Mrk 335. XMM spectra reveal a variable obscurer in this AGN,[20] which complicates measurements of intrinsic flux with NICER in the already background-dominated source.[21]

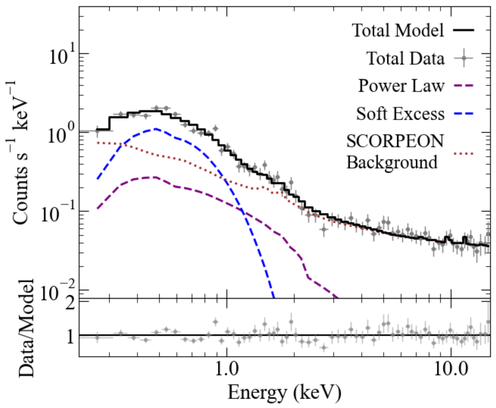

A NICER spectrum of Mrk 335 on MJD 58778. The AGN is fainter than the background above ~ 1 keV, despite normal background conditions.

References
[1] Partington, E.R. et al. 2025 ApJ 986 81
[2] Partington, E.R. et al. 2024 ApJ 977 77
[3] Peterson, B.M. et al. 1998 PASP 110 660
[4] Cackett, E. M. et al. 2020 ApJ 896 1
[5] Li, Y.-R et al. 2018, ApJ, 869 137
[6] Miller, J. A. et al. 2023, ApJ 95, 137
[7] Bentz, M. C., & Katz, S. 2015 PASP 127 67
[8] Prince, R. et al. 2025 MNRAS 541 642
[9] S. Hagen & C. Done 2023 MNRAS 521 251
[10] Peterson, B. M. et al. 2004 ApJ 613 682
[11] Cackett, E.M. et al. 2020 896 1
[12] Brotherton, M. B. et al. 2020 ApJ 905 77
[13] Partington, E.R. et al. 2023 ApJ 947 2
[14] Kara, E. et al 2021 ApJ 922 151
[15] Merritt, R. 2022 DOI:10.57709/29366502
[16] Bentz, M. C. et al. 2022 ApJ 934 168
[17] Waters, T. et al. 2022 ApJ 931 134
[18] Miller, J. M., et al. 2026 ApJL 1003 L34
[19] Lohfink, A. M. et al. 2016 ApJ 821 11
[20] Rogantini, D. et al. 2026 ApJ 1008 33
[21] Kara, E. et al. 2023 ApJ 947 62
[22] Abramowicz, M. A. et al. 1988 ApJ 332 646